Cosine law at the atomic scale: Toward realistic simulations of Knudsen diffusion

Franck Celestini* and Fabrice Mortessagne†
Laboratoire de Physique de la Matière Condensée, UMR 6622, CNRS and Université de Nice–Sophia Antipolis, Parc Valrose, 06108 Nice Cedex 2, France

(Received 2 August 2007; revised manuscript received 11 January 2008; published 8 February 2008)

We propose to reconsider the diffusion of atoms in the Knudsen regime in terms of a complex dynamical reflection process. By means of molecular dynamics simulations, we emphasize the asymptotic nature of the cosine law of reflection at the atomic scale, and carefully analyze the resulting strong correlations in the reflection events. A dynamical interpretation of the accommodation coefficient associated with the slip at the wall interface is also proposed. Finally, we show that the first two moments of the stochastic process of reflection depend nonuniformly on the incident angle.

DOI: 10.1103/PhysRevE.77.021202 PACS number(s): 47.45.Ab, 68.43.Jk, 83.10.Rs

A century ago, Knudsen proposed a model describing the diffusion of dilute gases through cylindrical pores [1]. The mean free path of the molecules being larger than the pore size, the transport properties are essentially driven by the collisions with the wall. In the Knudsen approach, based on the kinetic theory of gases, all rebounds were assumed to be governed by the diffusive Lambert cosine law of reflection [2]. Later, the model was improved by Smoluchowski who proposed, using Maxwell's theory, that only a fraction f of rebounds were diffuse, while the remaining $1-f$ were specular [3]. The physical situations addressed by these authors gained renewed interest due to the emerging applications in gas separation [4] and catalysis by means of new porous materials [5]. In order to achieve efficient processes a thorough understanding of the mechanisms involved in the transport of gas through a porous membrane is required (see Ref. [6] for a recent review). This problem has essentially been addressed by two distinct types of numerical simulation: billiardlike simulations (BLSs) and molecular dynamics (MD). In the first, the gas-wall interaction is introduced through *ad hoc* laws of reflection, disregarding microscopic mechanisms. Therefore, BLSs are more appropriate to describe the impact of the pore geometry on the transport properties at a macroscopic scale [7–9]. In MD, microscopic interactions are properly considered, the cost being a limitation in the spatial and time scales investigated by the simulations [10–12].

To combine the advantages of both kinds of simulation, one could extract from MD the realistic reflection law that would be finally incorporated in a BLS. A first step in this direction has recently been made by Arya *et al.* [13]. Using MD, these authors quantified the relationship between the phenomenological coefficient f and the parameters of the Lennard-Jones potential describing gas-wall interactions, namely, the wall structure and the interaction energy. Nonetheless, a realistic way of introducing f in a BLS has not been achieved yet.

In this paper we propose to fill the gap between MD and BL simulations. First, we show the robustness of the cosine law by successfully testing it against MD results. Then the velocity distribution functions are analytically derived and successfully compared to numerical results. We reexamine the cosine law of reflections, emphasizing its asymptotic nature. Through a careful analysis of the correlations between consecutive reflection events, we establish a relation between f and the range of the dynamical correlations. Finally, we present an analysis of the reflection law in terms of a complex stochastic process.

We use MD simulations to describe the trajectory of a particle through a two-dimensional slit pore, taking into account the atomistic structure of the walls (see Fig. 1). The equations of motion are integrated through a standard Verlet algorithm [14] with periodic boundary conditions in both directions. The two different interaction potentials, between the atoms composing the wall and between the diffusing particle and the atoms, are of the Lennard-Jones type: $V(r)=4\epsilon[(\sigma/r)^{12}-(\sigma/r)^{6}]$. We use a shifted force potential to guard against energy and force discontinuities at the cutoff radius $r_c=2.5\sigma$ [14]. For both potentials $\sigma=1$; for interactions between the wall atoms $\epsilon=1$ while ϵ takes values ranging from 0.005 to 0.5 for the particle-atom potential. The mass of the atoms is fixed to $m=1$. As a consequence, lengths, energies, and masses are respectively expressed in units of σ, ϵ, and m, and times in units of $\tau=m^{0.5}\sigma\epsilon^{-0.5}$.

The walls are composed of 141 atoms arranged in a triangular structure (see Fig. 1); the height of the pore is fixed

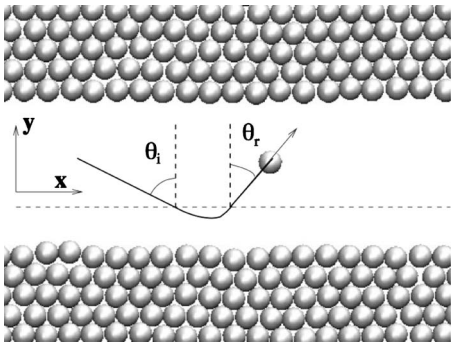

FIG. 1. Snapshot of the simulated system where a rebound event is schematically depicted. The dotted line shows the border between the ballistic and interacting regions.

*Franck.Celestini@unice.fr
†Fabrice.Mortessagne@unice.fr

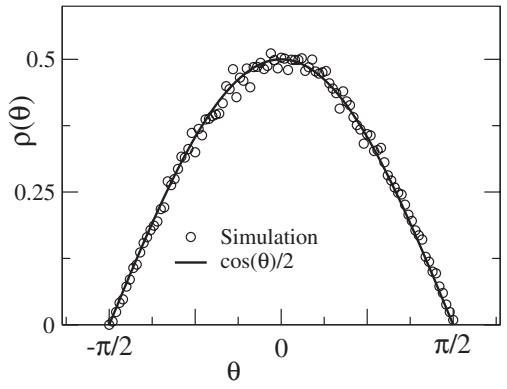

FIG. 2. Probability density function of the rebound angle. Simulation data (circles) obtained for $\epsilon=0.1$ are in complete agreement with the expected cosine law (1) (full line). The same agreement is observed whatever the value of ϵ.

to 6σ. Since the potential is of finite range, we can easily define the ballistic region, in the central part of the pore, where the diffusing particle does not interact with the walls. To characterize the "rebounds" we therefore record the particle positions and velocities at the borders of this region (see Fig. 1). The Boltzmann constant is set to unity and the temperature, expressed in units of energy, is fixed to $T=0.15$, a value for which the solid phase of the wall is stable. Once the system is in thermal equilibrium we perform simulations in the microcanonical ensemble. A typical run consists of 3×10^9 time steps ($\Delta t=10^{-3}$) during which we roughly compute from 10^5 to 4×10^5 rebounds on the walls, depending on the value of ϵ.

The probability density function of the reflection angles $\rho(\theta)$ obtained numerically through an averaging over 2×10^5 bounces and for $\epsilon=0.1$ is shown in Fig. 2. Our numerical results confirm the expected cosine law of reflection:

$$\rho(\theta)d\theta=\frac{1}{2}\cos\,\theta\,d\theta,\quad \rho(\sin\,\theta)d\,\sin\,\theta=\frac{1}{2}d\,\sin\,\theta. \quad (1)$$

The same remarkable agreement is observed for all the values of ϵ used in our simulations, showing the robustness of the cosine law. It is worth noting that relation (1) represents an asymptotic law (time $t\to\infty$) which does not preclude correlations between successive angles of reflection. One can even obtain such "ergodic" behavior with a purely specular law of reflection, for a nontrivial geometry of the surrounding walls. Indeed, in the limiting case of billiard problems, which constitute paradigmatic examples of Hamiltonian chaos, one generically obtains the cosine law of reflection, whereas incident and reflected angles are specularly related [15]. The role of short-time correlations between angles of reflection, which cannot be neglected, will be addressed in detail in the last part of the paper.

We use the cosine law as the starting point to derive analytically the other distribution functions describing the motion of the diffusing particle in the ballistic zone. As expected, our simulations show that the velocity component parallel to the surface, $v_x=v\,\sin\,\theta$, is a Gaussian random variable with variance given by the fixed temperature (for simplicity, the mass of the particle is 1):

$$\rho_x(v_x)=\frac{1}{\sqrt{2\pi T}}\exp\left(-\frac{v_x^2}{2T}\right). \quad (2)$$

The velocity can be described by two sets of random variables (v_x,v_y) or $(v,\sin\,\theta)$, whose distributions are related by

$$\rho(v,\sin\,\theta)=\left|\frac{\partial(v_x,v_y)}{\partial(v,\sin\,\theta)}\right|\rho(v_x,v_y)=\frac{v}{\cos\,\theta}\rho(v_x,v_y). \quad (3)$$

We numerically checked that v_x and v_y (or, equivalently, v and $\sin\,\theta$) are independent random variables: $\rho(v_x,v_y)=\rho_x(v_x)\rho_y(v_y)$ $[\rho(v,\sin\,\theta)=\rho_v(v)\rho_\theta(\sin\,\theta)]$. Thus, the distribution ρ_y can be obtained from the probability density of the modulus $\rho_v(v)=\int_{-1}^{1}d(\sin\,\theta)\rho(v,\sin\,\theta)$. From the normalization constraint $\int_0^\infty dv\;\rho_v=1$ one indeed obtains

$$\int_{-1}^{1}d(\sin\,\theta)\int_0^\infty dv\frac{v\rho(v\,\cos\,\theta)}{\cos\,\theta}\exp\left(-\frac{v^2\,\sin^2\,\theta}{2T}\right)=\sqrt{2\pi T}, \quad (4)$$

where we used the Maxwell-Boltzmann distribution (2). The solution of (4) is given by $\rho(v\,\cos\,\theta)=(v\,\cos\,\theta/T)\times\exp(-v^2\,\cos^2\,\theta/2T)$. Finally, we can assume for v_y the following distribution:

$$\rho_y(v_y)=\frac{v_y}{T}\exp\left(-\frac{v_y^2}{2T}\right). \quad (5)$$

Due to the nonsymmetric interactions experienced by the particle in the y direction, the corresponding velocity distribution (5) differs qualitatively from (2). Recall that (5) is fully compatible with the diffuse law of reflection (1). A similar expression to (5) was phenomenologically obtained by Arya *et al.* [13].

Knowing ρ_x and ρ_y, we are now able to write the explicit form of ρ_v:

$$\rho_v(v)=\sqrt{\frac{2}{\pi}}\frac{v^2}{T^{3/2}}\exp\left(-\frac{v^2}{2T}\right). \quad (6)$$

As expected from (5), it is clear that the modulus v does not obey the standard two-dimensional Maxwell distribution.[1] As expected from a microcanonical system, the motion of the particle in the ballistic zone and the walls is characterized by a Maxwellian velocity distribution. Expression (6) is successfully tested against the simulation results as shown in Fig. 3. Here again the agreement is quite remarkable whatever the values of ϵ. For comparison the two-dimensional (2D) Maxwell distribution is also shown in Fig. 3. Note that the mean value $\langle v\rangle=\sqrt{8T/\pi}$ deduced from (6) is around 20% smaller than the Maxwell mean value $\langle v_m\rangle=\sqrt{\pi T/2}$. We want to draw attention to the fact that distribution (6) should be used in BLSs of Knudsen diffusion. Indeed, the commonly

[1]For a 3D problem, we would have obtained $\rho_v(v)=(v^3/2T^2)\exp(-v^2/2T)$.

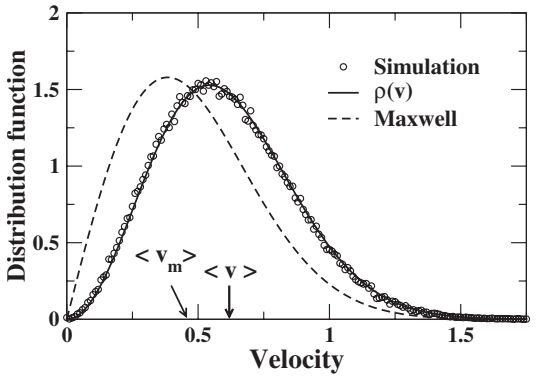

FIG. 3. Probability density function of the velocity modulus. Circles are simulation data; the full and dotted curves correspond, respectively, to $\rho_v(v)$ given in (6) and to the Maxwell distribution.

used Maxwell distribution leads to an underestimate of the diffusion constant.

We now turn to a thorough analysis of correlations between successive reflected angles in order to understand how the cosine law of reflection is asymptotically attained. We thus define the following function:

$$C(n) = 1 - \frac{\langle [\theta_p + (-1)^{n+1}\theta_{p+n}]^2 \rangle_p}{(\pi^2/2) - 4}. \tag{7}$$

$C(n)$ gives a measure of the correlation between two angles of reflection separated by n rebounds of the particle on the walls. By construction, $C(n)=1$ for a pure specular regime of reflections and $C(n)=0$ in the diffusive regime. The evolution of $C(n)$ for three values of ϵ is shown in Fig. 4. We observe that the expected convergence toward the diffusive limit as n increases is observed. We numerically verified that the mean resident time of the particle inside the interacting region increased with ϵ. As a consequence, one can see in Fig. 4 that the rate of convergence to $C=0$ increases with larger ϵ. But it is worth noting that $C(n)$ exhibits nonzero values for a significant number of bounces. The correlation functions exhibit an exponential behavior $C(n)=\exp(-n/n_c)$, where the characteristic number of rebounds n_c gives the range of the correlation: two angles of reflection separated by

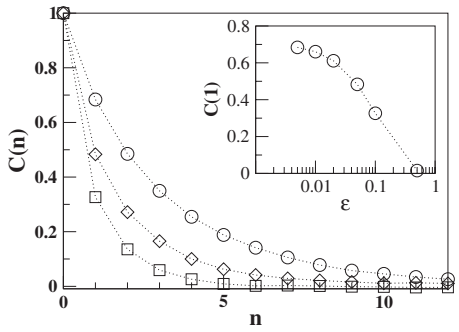

FIG. 4. Correlation function $C(n)$ represented for different values of ϵ. Circles, diamonds, and squares correspond to $\epsilon=0.005$, 0.02, and 0.1. Inset: $C(1)$ is plotted as a function of ϵ.

a small number of rebounds greater than n_c are uncorrelated. For the correlation functions shown in Fig. 4, n_c varies from 0.23, for the largest value of ϵ, to 2.92, for the smallest. Such a large number of "nondiffusive" (or "quasispecular") rebounds may drastically alter the transport process. This is what was phenomenologically taken into account in the Smoluchowsky model [3] by introducing fractions f and $1-f$ of atoms having diffuse and specular rebounds, respectively. This fraction f is called the tangential momentum accommodation coefficient and can be related to the slip coefficient at the wall [3,16]. Our approach gives an insight into the microscopic dynamics that generates the observed macroscopic behavior and provides an interpretation of the phenomenological coefficient. In order to mimic the observed correlations, one can indeed imagine a more realistic BLS where n_c rebounds are specular, after which the next rebound is diffuse and followed by another n_c specular rebound. Thus, the accommodation coefficient can be viewed as the inverse of the characteristic number of rebounds: $f \sim 1/n_c$.

Let us now focus on $C(1)$, which quantifies the loss of memory after a single bounce. The inset in Fig. 4 shows the evolution of this "instantaneous" correlation function with the strength of the potential. Even for the smallest value of ϵ the reflection is never truly specular [in this case $C(1)=1$] due to the atomic structure of the wall. As expected, for increasing values of ϵ $C(1)$ vanishes, indicating a complete randomization of the reflection events. This is clearly illustrated by looking at the motion of the particle for $\epsilon=0.1$, where the absence of correlations between incident and reflected angles is evident (see [17], video 1). Note that the diffusive behavior stems from the fact that for almost all rebounds the particle experiences, in the interacting zone, multiple collisions with wall atoms. This is no longer the case for $\epsilon=0.01$ (see [17], video 2) where a unique collision event generates the rebound.

Since the reflected angle is never completely diffusive or specular but something in between, the important quantity to know is the conditional probability $\rho(\theta_r|\theta_i)$ of rebounding with an angle θ_r, the incident angle θ_i being fixed. If we want to focus on the deviation from the specular regime, it is convenient to write $\theta_r=-\theta_i+\Delta\theta$ and therefore express the conditional probability as a set of distributions $\rho_{\theta_i}(\Delta\theta)$. We computed $\langle \Delta\theta(\theta_i)\rangle$ and $\langle \Delta\theta(\theta_i)^2\rangle$, the first and second moments of these distributions, and plot it for different values of ϵ in Fig. 5. In the case of a purely diffusive reflection, we expect

$$\langle \Delta\theta(\theta_i)\rangle = \theta_i, \tag{8}$$

$$\langle \Delta\theta(\theta_i)^2\rangle = \theta_i^2 + \pi^2/4 - 2. \tag{9}$$

As shown in Fig. 5, the diffusive behavior is recovered for the most attractive potential ($\epsilon=0.5$) considered in this study. The opposite case of purely specular reflections, characterized by $\langle \Delta\theta(\theta_i)\rangle=0$ and $\langle \Delta\theta(\theta_i)^2\rangle=0$, is never reached. Indeed, as discussed above when interpreting the fact that $C(1)\neq 1$ even for $\epsilon\to 0$, the wall structure precludes the emergence of a purely specular regime. In the intermediate regimes ($\epsilon=0.05, 0.005$), one can see that both moments

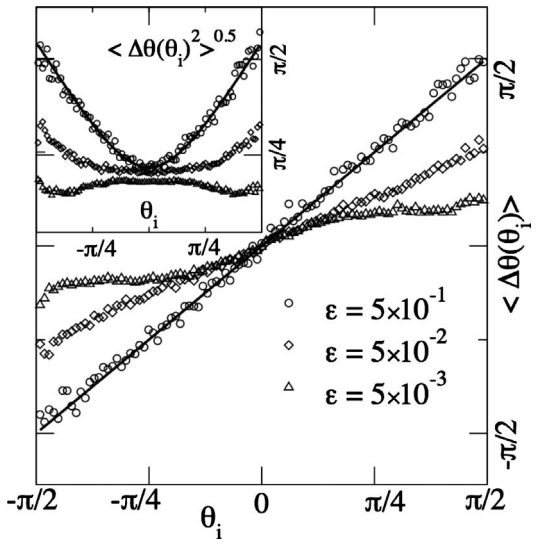

FIG. 5. First and second (inset) moments of the distributions $\rho_{\theta_i}(\Delta\theta)$. The full lines correspond to the purely diffusive regime. Circles, diamonds, and triangles correspond, respectively, to $\epsilon = 0.005$, 0.05, and 0.5.

nonuniformly depend on the incident angle, the nongeneric behavior being more important for the largest incident angles. Thus, we demonstrate here that the correlations between two successive rebounds are quantitatively sensitive to the value taken by the first rebound. We are currently developing an analytical description of such a complex behavior in the choice of the reflected angle in an improved BLS scheme.

In this paper, we have proposed additional insight into the so-called cosine law of reflection by means of MD simulations. We confirmed its validity at the atomic scale whatever the strength of the gas-wall interaction, but only as an asymptotic law. We examined two crude "ergodic" approximations in the studies of Knudsen diffusion, which (i) assume Maxwell velocity distribution functions and (ii) neglect the correlations between consecutive rebounds. We gave the correct distributions, Eqs. (5) and (6), actually involved in the Knudsen regime. By defining an appropriate correlation function (7), we carefully analyzed the strong correlations occurring in the dynamical process of reflection. We revealed a characteristic correlation rebound number n_c that has been linked to the commonly used accommodation coefficient f. Finally, we performed the complete characterization of the stochastic rebound process and emphasized the nontrivial dependence of the conditional probability $\rho(\theta_r|\theta_i)$ on the incident angle. This work should pave the way for new studies of Knudsen transport using improved BLS schemes as proposed in this paper.

We gratefully acknowledge fruitful discussions with A. ten Bosch. We also wish to thank G. Batrouni, A. ten Bosch, and S. Tanzilli for their careful reading of the manuscript.

[1] M. Knudsen, Ann. Phys. (Leipzig) **28**, 75 (1909).
[2] M. Knudsen, *The Kinetic Theory of Gases* (Methuen & Co., London, 1934).
[3] M. Smoluchowski, Ann. Phys. (Leipzig) **33**, 1559 (1910); E. H. Kennard, *Kinetic Theory of Gases* (McGraw-Hill, New York, 1938).
[4] V. Sotirchos and V. Burganos, MRS Bull. **24** (3), 41 (1999).
[5] M. E. Davis, Nature (London) **417**, 813 (2002).
[6] S. K. Bhatia, Adsorpt. Sci. Technol. **24**, 101 (2006).
[7] S. E. Albo, L. J. Broadbel, and R. Q. Snurr, AIChE J. **52**, 3679 (2006).
[8] R. Feres and G. Yablonsky, Chem. Eng. Sci. **61**, 7864 (2006).
[9] S. Zschiegner, S. Russ, A. Bunde, and J. Kärger, Europhys. Lett. **78**, 20001 (2007).
[10] A. I. Skoulidas, D. M. Ackerman, J. K. Johnson, and D. S. Sholl, Phys. Rev. Lett. **89**, 185901 (2002).
[11] S. Jakobtorweihen, M. G. Verbeek, C. P. Lowe, F. J. Keil, and B. Smit, Phys. Rev. Lett. **95**, 044501 (2005).
[12] S. K. Bhatia and D. Nicholson, J. Chem. Phys. **119**, 1719 (2003).
[13] G. Arya, H.-C. Chang, and E. J. Maginn, Mol. Simul. **29**, 697 (2003).
[14] M. P. Allen and D. J. Tildesley, *Computer Simulation of Liquids* (Clarendon Press, Oxford, 1987).
[15] F. Mortessagne, O. Legrand, and D. Sornette, Chaos **3**, 529 (1993).
[16] G. Arya, H.-C. Chang, and E. J. Maginn, Phys. Rev. Lett. **91**, 026102 (2003).
[17] See EPAPS Document No. E-PLEEE8-77-079802 for videos of a particle diffusing in a pore. For more information on EPAPS, see http://www.aip.org/pubservs/epaps.html.